ARTICLE

Tunable Band Gap in Hydrogenated Bilayer Graphene

Duminda K. Samarakoon and Xiao-Qian Wang*

Department of Physics and Center for Functional Nanoscale Materials, Clark Atlanta University, Atlanta, Georgia 30314

ABSTRACT We have studied the electronic structural characteristics of hydrogenated bilayer graphene under a perpendicular electric bias using first-principles density functional calculations. The bias voltage applied between the two hydrogenated graphene layers allows continuous tuning of the band gap and leads to transition from semiconducting to metallic state. Desorption of hydrogen from one layer in the chair conformation yields a ferromagnetic semiconductor with a tunable band gap. The implications of tailoring the band structure of biased system for future graphene-based device applications are discussed.

KEYWORDS: graphene · bilayer · hydrogenation · electric bias · density functional calculations

Graphene is a one-layer sheet of carbon with a structure that resembles chicken wire. Graphene has been proven to possess unique electronic and physical properties, such as the unconventional quantum Hall effect[1] and high carrier mobility at room temperature,[2−4] thereby holding potential for a wide range of applications including graphene transistors, integrated circuits, and biosensors.[1−4] The quantum Hall effect[5] and the associated strongly correlated electron systems have generated a tremendous impetus on the development of novel ideas in many-body physics like the existence of fractionally charged quasiparticles,[6] topological quantum numbers,[7] chiral Luttinger liquids,[8,9] composite fermion particles,[10,11] and Chern−Simons effective-field theories.[12,13] Bringing graphene up to the level of technologically relevant material, however, depends on improved understanding and control of the structural and electronic properties. Specifically, an energy gap can be engineered by introducing lateral confinement such as in graphene nanoribbons,[14−17] hydrogenated graphene,[18−20] or in biased bilayer graphene.[21−29] The engineering of band gaps generates a pathway for possible graphene-based nanoelectronic and nanophotonic devices.

The extremely high carrier mobility makes graphene an ideal material for nanoelectronic applications, especially in field-effect transistors.[2−4] Although graphene nanoribbon field-effect transistors have been shown to exhibit excellent properties,[14,16] mass production of graphene nanoribbon-based devices is beyond the capability of current lithography technology.[21] An alternative route to induce the formation of a band gap is through the hydrogenation of graphene.[18,19] The modification of the carbon bonds associated with the hydrogenation preserves the crystalline order of the lattice but leads to rehybridization of the carbon atoms from a planar sp^2 to a distorted sp^3 state.[20] Recent experimental studies have demonstrated reversible hydrogenation through heating and proceeding with dehydrogenation of the graphane to graphene.[18] On the other hand, bilayer graphene has attracted a great deal of attention recently. In bilayer graphene, the low energy excitations are one of the characteristics of massive chiral fermions, unlike Dirac fermions in graphene.[30] Most importantly, bilayer graphene can have a tunable gap *via* chemical doping or by applying an external gate voltage. In lieu of the increasing amount of experimental and theoretical studies of the bilayer graphene transistors,[31] the exploration of various modified bilayer systems could play a crucial role in future nanoelectronics applications.

Experimental advances have motivated our study of what could emerge if bilayer graphene were subjected to hydrogenation and electric bias. Here we present the corresponding results based on first-principles density functional calculations. Fully hydrogenated bilayer graphene is similar to the one-layer graphane in that the electronic

*Address correspondence to xwang@cau.edu.

Received for review April 15, 2010 and accepted June 3, 2010.

Published online June 10, 2010. 10.1021/nn1007868

properties change from metallic to the semiconductive due to the induced changes of functionalized carbon from sp^2 to sp^3 hybridization and the interlayer chemical bonding that stabilizes the hydrogenated structure.[32] We show that, with applied electric bias, the resultant energy gap can be tuned. Of particular interest are the effects associated with symmetry breaking due to the presence of an external electric field perpendicular to the hydrogenated bilayer graphene. Our work suggests a unique opportunity to tune the band gap of a ferromagnetic semiconductor with desorption of hydrogen from one layer in the chair conformation.

RESULTS AND DISCUSSION

While the opening and external tuning of energy gap between valence and conduction bands in Bernal stacking bilayer graphene[22,23] hold great potential for logic applications, switching off the conduction to a desirable level remains challenging in epitaxial graphene.[4] In this regard, it is of interest to investigate bilayer hydrogenated graphene that is semiconducting from the onset. Figure 1 depicts the fully and half hydrogenated chair and boat conformations. As can be seen from Figure 1, for the fully hydrogenated structures, a chemical bonding between the $A-B'$ sites stabilizes both chair and boat conformations. In the latter case, the chemical bonding induces a structural transformation that deviates from the pattern of Bernal stacking.

The geometry details are listed in Table 1 along with the calculated binding energy and band gap. Analogous to graphane from the one-layer fully hydrogenated graphene, the chair conformation[33,34] is the lowest energy conformation for fully hydrogenated bilayer, in agreement with previous first-principles density functional predictions.[20] Furthermore, the corresponding chemical bonding between the bilayer remains stable with the desorption of hydrogen in one layer, resulting in a slight increase of the interlayer bonding distance from 1.54 to 1.65 Å (Table 1). It is important to remark that, while the interlayer chemical bonding remains intact after desorption of hydrogens in one layer, the lowest energy configuration for one-sided hydrogenation is a boat conformation without the chemical bonding (Table 1). The crucial difference between the hydrogen desorption in one layer and the one-sided hydrogenation should be of particular interest in the forthcoming discussions.

There have been a number of theoretical studies on opening up a band gap in the gapless bilayer graphene if an electric field is applied perpendicularly.[35−39] The effect of the electric field can be studied by adding a potential *via* the nuclear charges. Our calculations show that the bilayer graphene opens a gap of ~0.23 eV by an electric bias of ~0.51 V/Å. This is in agreement with other theoretical predictions and experimental

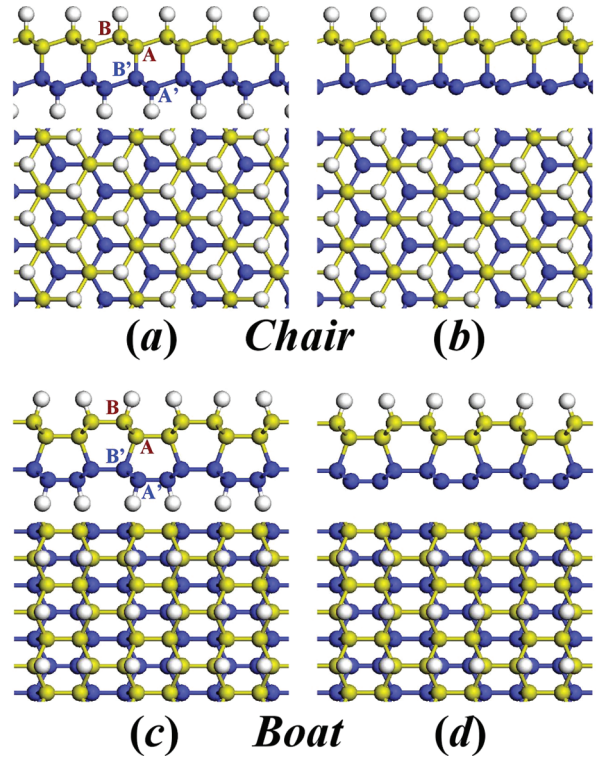

Figure 1. Side views of (a) fully hydrogenated and (b) semi-hydrogenated chair conformations of bilayer graphene. Top and side views of (c) fully hydrogenated and (d) semi-hydrogenated boat structures of bilayer graphene. Carbon atoms on top and on bottom layers are colored with gold and blue, respectively. Hydrogen atoms are colored with white.

observations.[26,38] However, when the electric bias is further increased, the gap in the bilayer system collapses, and the system turns back to metallic with induced interlayer bonding $A-B'$ reminiscent of the hydrogenated bilayer graphene. We show in Figure 2 the calculated band structures for bilayer graphane for chair conformation. As is readily observable from Figure 2, the band gap decreases monotonically from about 3.24 to 0 eV with increase of electric bias. The critical bias for the semiconducting to metallic transition is estimated to be 1.05 V/Å.

Shown in Figure 3 are the corresponding charge densities. In the absence of bias, the charge density dis-

TABLE 1. Calculated Binding Energy per Carbon Atom E_B, Band Gap E_g, and the Inter-Layer Bond Length l For Chair and Boat Conformations of Fully Hydrogenated and Semi-Hydrogenated Graphene, Respectively. Labels I and II Refer to Boat Conformations with and without Interlayer Bonding, Respectively

structure	E_B (eV)	E_g (eV)	l (Å)
fully hydrogenated chair	−12.00	3.24	1.54
fully hydrogenated boat	−11.93	2.92	1.54
semi-hydrogenated chair	−10.55	0.54	1.65
semi-hydrogenated boat I	−10.79	2.35	1.63
semi-hydrogenated boat II	−10.85	0.50	3.26

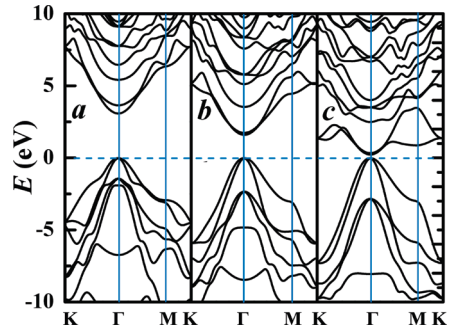

Figure 2. Calculated band structure of fully hydrogenated graphene in chair conformation with (a) no electric bias, (b) 0.39 V/Å electric bias, and (c) 1.03 V/Å electric bias; $K = (\pi/3a, 2\pi/3a)$, $M = (0, \pi/2a)$, where $a = 2.50$ Å. The valence band maximum is set to 0 eV.

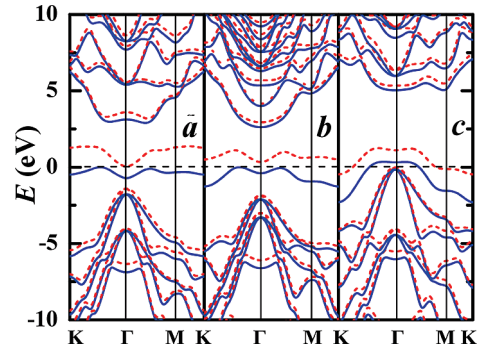

Figure 4. Calculated band structure for semi-hydrogenated bilayer graphene in chair conformation with (a) −0.26 V/Å electric bias, (b) no electric bias, and (c) 0.39 V/Å electric bias. The red and blue curves represent spin-up and spin-down components, respectively.

tributions are symmetrical in both conduction and valence bands. With the application of an electric bias, charge transfer in the conduction and valence bands acts in a concerted fashion, resulting in charge accumulation and depletion in the conduction and valence bands, respectively.

It is worth noting that there are no explicit magnetic states in fully hydrogenated bilayer graphene. This indicates that the chemical bonds and the electric-field-induced dipole−dipole interaction do not lead to unpaired spins. The unpaired spins can be generated through desorption of the hydrogen in one layer or through one-sided absorption. The latter scenario is particulary interesting in that one can take advantage of the electric field that generates chemical bonding prior to the hydrogenation. However, the chemical bonding is simultaneously breaking when the electric bias is switched off. We have carefully studied both scenarios. The desorption of the fully hydrogenated chair conformation can be readily confirmed. However, the one-sided hydrogenation is much more involved due to

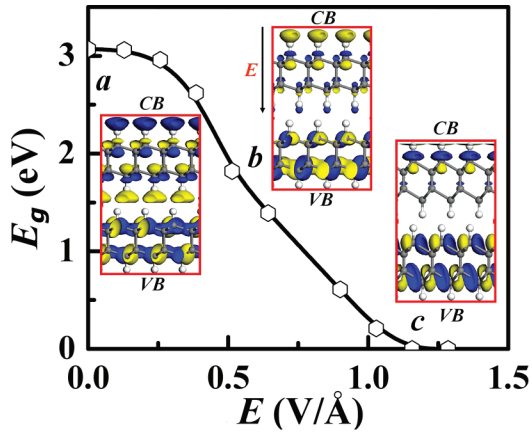

Figure 3. Calculated dependence of band gap on perpendicular applied electric bias for the bilayer graphane in chair conformation: (a) no bias, (b) 0.39 V/Å electric bias, and (c) 1.03 V/Å electric bias. Insets: extracted charge density distribution at the band center (Γ point) of the corresponding conduction and valence band states. The isovalue is 0.025 au.

the crucial dependence of the hydrogenation patterns, which favors a boat conformation at large hydrogen coverage that is nonmagnetic.

Hydrogenation of graphene is reversible, providing the flexibility to manipulate its coverage.[18] The desorption of the hydrogen atoms from one side of graphane will result in a semi-hydrogenated bilayer graphene, which is the counterpart of the monolayer "graphone".[40] Graphone is a ferromagnetic semiconductor with a small indirect gap attributed to the breaking of the delocalized π-bonding network of graphene delocalization, which is associated with localized and unpaired electrons.[40,41] Shown in Figure 4 are the calculated band structures for one-sided hydrogenated bilayer graphene under electric bias. For semi-hydrogenated bilayer graphene, there is an indirect band gap about 0.54 eV (Figure 4b). This changes to metallic for biased voltages below −0.26 V/Å (Figure 4a) or above 0.39 V/Å (Figure 4c).

Our results show that the bilayer counterpart of graphone is ferromagnetic. Partial saturation of carbon atoms in hydrogenated graphene breaks its π-bonding network, resulting in localized and unpaired electrons.[40] The magnetic moments couple ferromagnetically with the semi-hydrogenated chair conformation. Electronic structure changes by partial hydrogenation as well. The semi-hydrogenated graphene of chair conformation is an indirect band gap semiconductor with a small band gap, very different from the original graphene and graphane. We illustrate in Figure 5 the dependence of the spin-polarized bands of semi-hydrogenated bilayer graphene with the positive and negative bias. The energy gap decreases monotonically with the electric field by characterizing the properties from magnetic semiconductor with a small gap to a metal with a zero gap. In contrast to fully hydrogenated bilayer graphene, the changes in the gap are no longer symmetrical with the negative and positive bias. Apart from the partial shifts of the spin density to

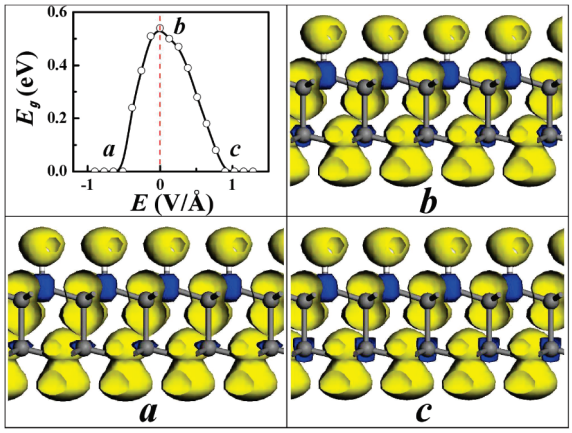

Figure 5. Calculated band gaps of semi-hydrogenated bilayer graphene in chair structure with (a) −0.26 V/Å electric bias, (b) no bias, and (c) 0.39 V/Å electric bias. Insets: extracted spin density distribution at the band center (Γ point) of the corresponding conduction and valence states. The isovalue is 0.025 au.

the bottom layer, closer scrutiny reveals a paucity of modifications of the spin density distribution when the applied electric field goes from negative to positive bias. In connection to the spin density shift, the band dispersion changes from nearly flat to pronounced dispersion near the band edge at *K*, which leads to the change of the indirect gaps.

CONCLUSIONS

In summary, we have studied the electronic characteristics of biased bilayer graphane. The resultant hydrocarbon compound, bilayer graphane, can be modified into new materials, fine-tuning its electronic properties. These studies have revealed increasingly fertile possibilities in hydrogen storage and two-dimensional electronics. These novel semiconducting behaviors result from a peculiar, effective transformation of sp^2 to sp^3 carbon and allow a continuously tunable band gap in biased bilayer graphane. A bilayer version can deliver yet another interesting feature of tunable band gap. This discovery paves the way for new electronic devices, from lasers that change color to electronic circuits that can rearrange themselves. The tunable band gap, which generally determines transport and optical properties, will enable flexibility and optimization of graphene-based nanodevices. Moreover, our proposed desorption of hydrogen from one layer, coupled with controlled hydrogen vacancy distribution and patterned hydrogenation, could provide a promising route to realize a ferromagnetic semiconductor in view of the crucial structural difference between monolayer graphone and the bilayer semihydrogenated graphene.

METHODS

The structural and electronic properties were investigated using first-principles density functional calculations.[42] Our first-principles calculations are based on spin-polarized density functional theory with local density approximation (LDA) for exchange-correlation potential.[43] A supercell with a vacuum space of 16 Å normal to the graphene plane was used. A kinetic energy change of 3×10^{-4} eV in the orbital basis and appropriate Monchorst−Pack *k*-point grids of $6 \times 6 \times 1$ were sufficient to converge the integration of the charge density. The optimization of atomic positions proceeds until the change in energy is less than 1×10^{-6} eV per cell. Although the LDA approach systematically underestimates the band gaps, we are primarily interested in the relative stability of the conformations and the electric field effects. While calculations based on hybrid functionals or many-body GW approaches can rectify the gaps (the rectified gap is 5.2−5.4 eV *vs* the LDA result of 3.6 eV for graphane),[26,34] the implementation of the corresponding electric-field effect is cumbersome. The LDA approach is expected to provide qualitatively correct pictures and remains the popular choice for investigations of electric-field effects.[26] Another reason for choosing LDA is attributed to the fact that generalized gradient approximation (GGA) leads to weak bonding between graphene layers and yields excessively large values of bilayer distance. By contrast, LDA calculation gives rise to a bilayer distance of ~3.3 Å, in good conformity with the results of graphite.[44]

Acknowledgment. This work was supported by the National Science Foundation (Grant DMR-0934142), Army Research Office (Grant W911NF-06-1-0442), and Air Force Office of Scientific Research (Grant FA9550-10-1-0254).

REFERENCES AND NOTES

1. Zhang, Y.; Jiang, Z.; Small, J. P.; Purewal, M. S.; Tan, Y.-W.; Fazlollahi, M.; Chudow, J. D.; Jaszczak, J. A.; Stormer, H. L.; Kim, P. Landau-Level Splitting in Graphene in High Magnetic Fields. *Phys. Rev. Lett.* **2006**, *96*, 136806.
2. Novoselov, K. S.; Geim, A. K.; Morozov, S. V.; Jiang, D.; Zhang, Y.; Dubonos, S. V.; Grigorieva, I. V.; Firsov, A. A. Electric Field Effect in Atomically Thin Carbon Films. *Science* **2004**, *306*, 666.
3. Berger, C.; Song, Z.; Li, X.; Wu, X.; Brown, N.; Naud, C.; Mayou, D.; Li, T.; Hass, J.; Marchenkov, A. N.; *et al.* Electronic Confinement and Coherence in Patterned Epitaxial Graphene. *Science* **2006**, *312*, 1191.
4. Neto, A. H. C.; Guinea, F.; Peres, N. M. R.; Novoselov, K. S.; Geim, A. K. The Electronic Properties of Graphene. *Rev. Mod. Phys.* **2009**, *81*, 109.
5. Tsui, D. C.; Stormer, H. L.; Gossard, A. C. Two-Dimensional Magnetotransport in the Extreme Quantum Limit. *Phys. Rev. Lett.* **1982**, *48*, 1559.
6. Laughlin, R. B. Anomalous Quantum Hall Effect: An Incompressible Quantum Fluid with Fractionally Charged Excitations. *Phys. Rev. Lett.* **1983**, *50*, 1395.
7. Thouless, D. J. *Topological Quantum Numbers in Nonrelativistic Physics*; World Scientic: Singapore, 1998.
8. Wen, X. G. Gapless Boundary Excitations in the Quantum Hall States and in the Chiral Spin States. *Phys. Rev. B* **1991**, *43*, 11025.
9. Wen, X. G. Electrodynamical Properties of Gapless Edge Excitations in the Fractional Quantum Hall States. *Phys. Rev. Lett.* **1990**, *64*, 2206.
10. Jain, J. K. Composite-Fermion Approach for the Fractional Quantum Hall Effect. *Phys. Rev. Lett.* **1989**, *63*, 199.
11. Ciftja, O. The Fermi-Sea-like Limit of the Composite Fermion Wave Function. *Eur. Phys. J. B* **2000**, *13*, 671.
12. Halperin, B. I. Theory of the Half-Filled Landau Level. *Phys. Rev. B* **1993**, *47*, 7312.
13. Ciftja, O.; Wexler, C. Energy Gaps for Fractional Quantum Hall States Described by a Chern−Simons Composite Fermion Wavefunction. *Eur. Phys. J. B* **2001**, *23*, 437.

14. Li, X.; Wang, X.; Zhang, L.; Lee, S.; Dai, H. Chemically Derived, Ultrasmooth Graphene Nanoribbon Semiconductors. *Science* **2008**, *319*, 1229.
15. White, C. T.; Li, J.; Gunlycke, D.; Mintmire, J. W. Hidden One-Electron Interactions in Carbon Nanotubes Revealed in Graphene Nanostrips. *Nano Lett.* **2007**, *7*, 825.
16. Wang, X.; Ouyang, Y.; Li, X.; Wang, H.; Guo, J.; Dai, H. Room-Temperature All-Semiconducting Sub-10-nm Graphene Nanoribbon Field-Effect Transistors. *Phys. Rev. Lett.* **2008**, *100*, 206803.
17. Nduwimana, A.; Wang, X.-Q. Energy Gaps in Supramolecular Functionalized Graphene Nanoribbons. *ACS Nano* **2009**, *3*, 1995.
18. Elias, D. C.; Nair, R. R.; Mohiuddin, T. M. G.; Morozov, S. V.; Blake, P.; Halsall, M. P.; Ferrari, A. C.; Boukhvalov, D. W.; Katsnelson, M. I.; Geim, A. K.; *et al.* Control of Graphene's Properties by Reversible Hydrogenation: Evidence for Graphane. *Science* **2009**, *323*, 610.
19. Guisinger, N. P.; Rutter, G. M.; Crain, J. N.; First, P. N.; Stroscio, J. A. Exposure of Epitaxial Graphene on SiC(0001) to Atomic Hydrogen. *Nano Lett.* **2009**, *9*, 1462.
20. Sofo, J. O.; Chaudhari, A. S.; Barber, G. D. Graphane: A Two-Dimensional Hydrocarbon. *Phys. Rev. B* **2007**, *75*, 153401.
21. Nilsson, J.; Neto, A. H. C.; Guinea, F.; Peres, N. M. R. Electronic Properties of Bilayer and Multilayer Graphene. *Phys. Rev. B* **2008**, *78*, 045405.
22. McCann, E. Asymmetry Gap in the Electronic Band Structure of Bilayer Graphene. *Phys. Rev. B* **2006**, *74*, 161403.
23. Ohta, T.; Bostwick, A; Seyller, T.; Horn, K.; Rotenberg, E. Controlling the Electronic Structure of Bilayer Graphene. *Science* **2006**, *313*, 951.
24. Oostinga, J. B.; Heersche, H. B.; Liu, X.; Morpurgo, A. F.; Vandersypen, L. M. Gate-Induced Insulating State in Bilayer Graphene Devices. *Nat. Mater.* **2008**, *7*, 151.
25. Castro, E. V.; Novoselov, K. S.; Morozov, S. V.; Peres, N. M. R.; dos Santos, J. M. B. L.; Nilsson, J.; Guinea, F.; Geim, A. K.; Neto, A. H. C. Biased Bilayer Graphene: Semiconductor with a Gap Tunable by the Electric Field Effect. *Phys. Rev. Lett.* **2007**, *99*, 216802.
26. Zhang, Y.; Tang, T.-T.; Girit, C.; Hao, Z.; Martin, M. C.; Zettl, A.; Crommie, M. F.; Shen, Y. R.; Wang, F. Direct Observation of a Widely Tunable Bandgap in Bilayer Graphene. *Nature* **2009**, *459*, 820.
27. Mak, K. F.; Lui, C. H.; Shan, J.; Heinz, T. F. Observation of an Electric-Field-Induced Band Gap in Bilayer Graphene by Infrared Spectroscopy. *Phys. Rev. Lett.* **2009**, *102*, 256405.
28. Min, H.; Sahu, B.; Banerjee, S. K.; MacDonald, A. H. *Ab Initio* Theory of Gate Induced Gaps in Graphene Bilayers. *Phys. Rev. B* **2007**, *75*, 155115.
29. Castro, E. V.; Peres, N. M. R.; dos Santos, J. M. B. L.; Guinea, F.; Neto, A. H. C. Bilayer Graphene: Gap Tunability and Edge Properties. *J. Phys.: Conf. Ser.* **2008**, *129*, 012002.
30. Novoselov, K. S.; Geim, A. K.; Morozov, S. V.; Jiang, D.; Katsnelson, M. I.; Grigorieva, I. V.; Dubonos, S. V.; Firsov, A. A. Two-Dimensional Gas of Massless Dirac Fermions in Graphene. *Nature* **2005**, *438*, 197.
31. Xia, F.; Farmer, D. B.; Lin, Y.-M.; Avouris, P. Graphene Field-Effect Transistors with High On/Off Current Ratio and Large Transport Band Gap at Room Temperature. *Nano Lett.* **2010**, *10*, 715.
32. Leenaerts, O.; Partoens, B.; Peeters, F. M. Hydrogenation of Bilayer Graphene and the Formation of Bilayer Graphane from First Principles. *Phys. Rev. B* **2009**, *80*, 245422.
33. Flores, M. Z. S.; Autreto, P. A. S.; Legoas, S. B.; Galvao, D. S. Graphene to Graphane: A Theoretical Study. *Nanotechnology* **2009**, *20*, 465704.
34. Samarakoon, D. K.; Wang, X.-Q. Chair and Twisted-Boat Membranes in Hydrogenated Graphene. *ACS Nano* **2009**, *3*, 4017.
35. Liu, L.; Shen, Z. Bandgap Engineering of Graphene: A Density Functional Theory Study. *Appl. Phys. Lett.* **2009**, *95*, 252104.
36. Giovannetti, G.; Khomyakov, P. A.; Brocks, G.; Kelly, P. J.; van den Brink, J. Substrate-Induced Band Gap in Graphene on Hexagonal Boron Nitride: *Ab Initio* Density Functional Calculations. *Phys. Rev. B* **2007**, *76*, 073103.
37. Avetisyan, A. A.; Partoens, B.; Peeters, F. M. Electric Field Tuning of the Band Gap in Graphene Multilayers. *Phys. Rev. B* **2009**, *79*, 035421.
38. Avetisyan, A. A.; Partoens, B.; Peeters, F. M. Electric-Field Control of the Band Gap and Fermi Energy in Graphene Multilayers by Top and Back Gates. *Phys. Rev. B* **2009**, *80*, 195401.
39. Grüneis, A.; Attaccalite, C.; Wirtz, L.; Shiozawa, H.; Saito, R.; Pichler, T.; Rubio, A. Tight-Binding Description of the Quasiparticle Dispersion of Graphite and Few-Layer Graphene. *Phys. Rev. B* **2008**, *78*, 205425.
40. Zhou, J.; Wang, Q.; Sun, Q.; Chen, X. S.; Kawazoe, Y.; Jena, P. Ferromagnetism in Semihydrogenated Graphene Sheet. *Nano Lett.* **2009**, *9*, 3867.
41. Boukhvalov, D. W.; Katsnelson, M. I.; Lichtenstein, A. I. Hydrogen on Graphene: Electronic Structure, Total Energy, Structural Distortions and Magnetism from First-Principles Calculations. *Phys. Rev. B* **2008**, *77*, 035427.
42. *DMol$_3$*; Accelrys Software Inc.: San Diego, CA, 2010.
43. Vosko, S. H.; Wilk, L.; Nusair, M. Accurate Spin-Dependent Electron Liquid Correlation Energies for Local Spin Density Calculations: A Critical Analysis. *Can. J. Phys.* **1980**, *58*, 1200.
44. Partoens, B.; Peeters, F. M. From Graphene to Graphite: Electronic Structure around the K Point. *Phys. Rev. B* **2006**, *74*, 075404.